

Gravitational waves from oscillating accretion tori: Comparison between different approaches

Alessandro Nagar^{1,2}, José A. Font¹, Olindo Zanotti¹ and Roberto De Pietri³

¹*Departament d'Astronomia i Astrofísica, Universitat de València,*

Edifici d'Investigació, Dr. Moliner 50, 46100 Burjassot (València), Spain

²*Dipartimento di Fisica, Politecnico di Torino, Corso Duca degli Abruzzi 23, 10129 Torino, Italy*

³*Dipartimento di Fisica, Università di Parma, Parco Area delle Scienze 7a, 43100, Parma, Italy*

(Dated: June 19, 2018)

Quasi-periodic oscillations of high density thick accretion disks orbiting a Schwarzschild black hole have been recently addressed as interesting sources of gravitational waves. The aim of this paper is to compare the gravitational waveforms emitted from these sources when computed using (variations of) the standard quadrupole formula and gauge-invariant metric perturbation theory. To this goal we evolve representative disk models using an existing general relativistic hydrodynamics code which has been previously employed in investigations of such astrophysical systems. Two are the main results of this work: First, for stable and marginally stable disks, no excitation of the black hole quasi-normal modes is found. Secondly, we provide a simple, relativistic modification of the Newtonian quadrupole formula which, in certain regimes, yields excellent agreement with the perturbative approach. This holds true as long as back-scattering of GWs is negligible. Otherwise, any functional form of the quadrupole formula yields systematic errors $\sim 10\%$.

PACS numbers: 04.30.Db, 95.30.Lz, 98.62.Mw

Quasi-periodic oscillations of axisymmetric thick accretion disks or tori orbiting around a black hole have been recently addressed as promising sources of gravitational waves (GWs) [1]. In Ref. [1] the GW signals were computed by means of the quadrupole stress formula within the Newtonian approximation, as it is commonly done in the literature [2, 3, 4, 5, 6]. The purpose of the present article is to compare the gravitational waveforms computed using the quadrupole formalism with those obtained from the theory of (gauge-invariant) gravitational metric perturbations of Schwarzschild spacetime, which amounts to solve (in the time domain) the inhomogeneous even- (Zerilli-Moncrief) and odd-parity (Regge-Wheeler) master equations [7, 8, 9]. Since our interest is on the comparison between the two approaches, we shall concentrate on even-parity perturbations only. We note that similar investigations have been reported by [6] in the context of oscillations of neutron stars, and by [10] for orbiting particles around a Schwarzschild black hole.

In order to perform such a comparison we use the same physical setup of [1], namely a relativistic thick accretion disk undergoing oscillations induced by suitable initial perturbations of an equilibrium configuration. A number of restrictive hypothesis are assumed in our computational framework which, however, are valid as long as the mass of the disk μ is much smaller than the mass of the black hole M . In such a case, the self-gravity of the disk and the radiation reaction effects can be neglected. We assume thus that the spacetime metric $\bar{g}_{\mu\nu}$ is described by the Schwarzschild metric $g_{\mu\nu}$ plus a non-spherical perturbation $h_{\mu\nu}$. As a result of the spherical symmetry, $h_{\mu\nu}$ can be expanded in seven even-parity and

three odd-parity multipoles

$$\bar{g}_{\mu\nu} = g_{\mu\nu} + \sum_{l=2}^{\infty} \sum_{m=-l}^l (h_{\mu\nu}^{\ell m})^{(e)} + (h_{\mu\nu}^{\ell m})^{(o)}, \quad (1)$$

with the even multipoles transforming as $(-1)^l$ and the odd as $(-1)^{l+1}$ under a parity transformation $(\theta, \varphi) \rightarrow (\pi - \theta, \pi + \varphi)$. The presence of a fluid matter disk around the black hole is accounted through a “source” term in the linearized Einstein’s equations, represented by a stress energy tensor $t_{\mu\nu}$ which can be expanded in multipoles as well (see [11, 12] for details). By taking suitable combinations of the metric multipoles, it is possible to define an even-parity $Z^{\ell m}$ (Zerilli-Moncrief) and an odd-parity $\Psi^{\ell m}$ (Regge-Wheeler) gauge-invariant master function. The linearized Einstein’s equations for the even-parity part reduce to the Zerilli-Moncrief equation in $Z^{\ell m}$

$$Z_{,tt}^{\ell m} - Z_{,r_*r_*}^{\ell m} + V_l^{(e)} Z^{\ell m} = S_z^{\ell m}, \quad (2)$$

where $r_* = r + 2M \log[r/(2M) - 1]$ is the Regge-Wheeler tortoise coordinate and

$$V_l^{(e)} = \left(1 - \frac{2M}{r}\right) \times \frac{\lambda(\lambda - 2)^2 r^3 + 6(\lambda - 2)^2 M r^2 + 36(\lambda - 2) M^2 r + 72 M^3}{r^3 [(\lambda - 2)r + 6M]^2} \quad (3)$$

is the Zerilli potential, with $\lambda = l(l + 1)$. Explicit expression for the source $S_z^{\ell m}$, in the gauge-invariant formalism of Gerlach-Sengupta [13], can be found in Refs. [11, 12]. In the wave-zone (i.e. for large r) it can be shown that the even-parity GW amplitude reads (see e.g. [12] and

TABLE I: Marginally stable (A, C) and stable (B, D) constant angular momentum thick disks orbiting around a Schwarzschild black hole of mass $M = 2.5M_\odot$. From left to right the columns report the name of the model, the number of radial and polar grid zones used in the simulations, the disk-to-hole mass ratio, the polytropic constant κ of the isentropic equation of state (EOS) $p = \kappa\rho^\gamma$ with $\gamma = 4/3$, the value of the specific angular momentum l , the position of the cusp r_{cusp} and of the center r_{center} of the disk, the density at the center ρ_c , the location of the inner (r_{in}) and outer (r_{out}) disk boundaries, the linear size in the equatorial plane L , the orbital period of the center t_{orb} , the value of the potential barrier ΔW , and the magnitude of the perturbation parameter η . The inner and outer radii of the computational domain are $r_{\text{min}} = 2.1$ (for all models) and $r_{\text{max}} = 18$ (A), 20 (B and C), and 40 (D). All radii are given in units of M .

Model	N_r	N_θ	μ/M	κ (cgs)	l	r_{cusp}	r_{center}	ρ_c (cgs)	r_{in}	r_{out}	L (km)	t_{orb} (ms)	ΔW	η
A	320	150	0.10	3.01×10^{13}	3.75	4.835	7.720	3.58×10^{13}	4.83	11.57	24.87	1.66	0	0.1
B	300	150	0.02	3.58×10^{13}	3.75	4.835	7.720	1.39×10^{13}	5.81	10.32	16.65	1.66	-0.002	0.01
C	300	150	0.10	9.60×10^{13}	3.80	4.576	8.352	1.15×10^{13}	4.57	15.89	41.76	1.86	0	0.01
D	300	150	0.01	6.19×10^{14}	3.95	4.107	9.971	2.83×10^{11}	5.49	29.08	87.09	2.43	-0.015	0.02

references therein)

$$h_+ - ih_\times = \frac{1}{2r} \sum_{l=2}^{\infty} \sum_{m=-l}^l Z^{\ell m} \sqrt{\frac{(l+2)!}{(l-2)!}} {}_{-2}Y^{\ell m}(\theta, \varphi), \quad (4)$$

where ${}_{-2}Y^{\ell m}(\theta, \varphi)$ are the $s = -2$ spin-weighted spherical harmonics. In axisymmetry ($m = 0$)

$$h_+ = \frac{1}{2r} \sum_{l=2}^{\infty} Z^{l0} W^{l0}, \quad (5)$$

where $W^{l0} = Y_{\theta\theta}^{l0} - \cot\theta Y_{\theta}^{l0}$, and $h_\times = 0$. The total energy radiated in GWs is defined by

$$E^{l0} = \int_0^\infty \left(\frac{dE}{d\omega} \right)^{l0} d\omega = \frac{1}{64\pi^2} \frac{(l+2)!}{(l-2)!} \int_0^\infty \omega^2 |\tilde{Z}(\omega, r)|^2 d\omega, \quad (6)$$

where we have introduced the Fourier transform $\tilde{Z}(\omega, r) = \int_{-\infty}^\infty e^{-i\omega t} Z(t, r) dt$, with $\omega = 2\pi f$ and $Z \equiv Z^{l0}$. In the following we focus our discussion on the $l = 2$ multipole where $W^{20} = \sqrt{45/(4\pi)} \sin^2\theta$.

The equilibrium accretion disks that we use as initial models for our simulations, and whose hydrodynamics is accounted for in the source terms of Eq. (2), are built by solving the relativistic Bernoulli equation as described in [14]. We only recall here that the tori are isentropic, non-Keplerian (thick) disks with a cusp on the equatorial plane, through which matter can accrete onto the black hole provided there is some departure from hydrostatic equilibrium. For simplicity, we only consider initial models with a uniform radial distribution of the specific angular momentum, a fact which guarantees that the radial location of the cusp is always smaller than the marginally stable orbit. Despite constant specific angular momentum disks do not represent physical tori, being dynamically unstable against nonaxisymmetric instabilities, such a simple model is still appropriate for our

purpose of testing the quadrupole formula (see [14] for details on improved models of equilibrium tori). The geometrical structure of the equipotential surfaces of the tori resembles that of the Roche lobes of a binary system. In particular, by varying the value of the potential barrier $\Delta W = W_{\text{in}} - W_{\text{cusp}}$ at the inner edge of the disk, it is possible to build either a stable configuration corresponding to a torus inside its Roche lobe ($\Delta W < 0$), or a torus overflowing its Roche lobe ($\Delta W > 0$) and therefore accreting onto the black hole. The case $\Delta W = 0$ corresponds to the marginally stable case.

In the present work we deal with models which are stable or marginally stable with respect to the runaway instability (see e.g. [14] and references therein). Table I lists the main properties of the models considered. The mass of the black hole is $M = 2.5M_\odot$, and disks with different disk-to-hole mass ratio μ/M are considered. In all cases, but particularly for models B and D, the disk represents a small perturbation to the gravitational field of the black hole. Models A and B share the same location of the center and the cusp (i.e. have the same equipotential surfaces), but differ in the total mass μ and in the value of the potential gap ΔW . In order to induce periodic oscillations of the disks we follow the same procedure of [1] and introduce a small radial velocity perturbation, parameterizing its strength in the form $v_r = \eta v_r^{\text{sph}}$, where v_r^{sph} is the (stationary) radial velocity of the spherically symmetric low density atmosphere surrounding the torus. The values of the perturbation parameter chosen are typically in the interval $\eta \in [0.01, 0.1]$. This produces low mass accretion rates (see below) and validates the assumption of a “fixed” background spacetime. The initial data are evolved in time using an axisymmetric general relativistic hydrodynamics code based on the conservative formulation of the equations, whose accuracy has been assessed in earlier investigations [1, 11, 14]. The computational (r, θ) -grid used in the simulations has non-uniform radial spacing and equidistant polar spacing. Table I reports the number of grid zones employed for each model.

It needs to be mentioned that setting up the initial data

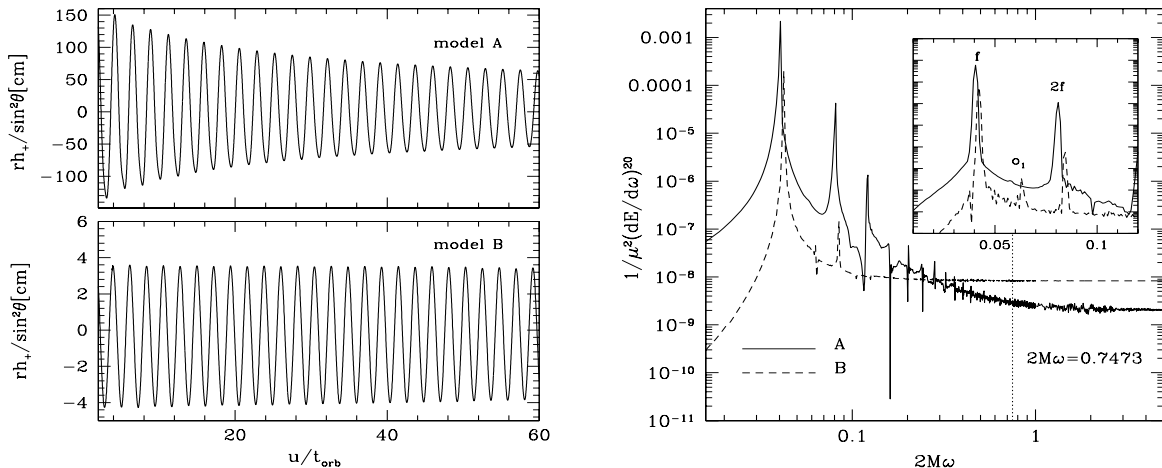


FIG. 1: *Left panel:* Time evolution of the $l = 2, m = 0$ GWs for models A and B, computed using the Zerilli-Moncrief equation. The first 60 periods of a $t = 100t_{\text{orb}}$ simulation are shown. The oscillatory pattern in the waveforms is the response of the quasi-periodic oscillations of the disks. *Right panel:* Energy spectra for model A (solid line) and B (dashed line). Only fluid p -modes are visible in the spectra (enlarged in the inset, where a Hamming filter was used) which show no evidence of the excitation of the fundamental QNM of the black hole (its frequency is indicated by a vertical dotted line at $2M\omega = 0.7473$).

for even-parity perturbations requires some care [11], as the initial profile of Z and $Z_{,t}$ should be obtained by solving the (linearized) Hamiltonian and momentum constraints with matter sources, respectively. When this is not done, an initial unphysical burst of gravitational radiation is produced, which may cause the excitation of the black hole quasi-normal modes (QNM) and hide physical effects if these were to happen on a comparable timescale. However, this is not the case in our simulations as the timescale of the oscillations of the disk is much larger than the decay time of the black hole QNM. Hence, once the initial data have been evolved for a sufficient time (roughly a couple of orbital periods) the gravitational waveforms remain entirely unaffected by the initial GW content. In practice, we choose for the initial profile of Z a $l = 2$ time-symmetric stationary multipole by solving Eq. (2) as an ODE with $Z_{,tt} = 0$.

The left panel of Fig. 1 shows the $l = 2$ gravitational waveforms extracted for models A and B through the Zerilli-Moncrief equation (at $r_{\text{obs}} = 400M$) as a function of the observer retarded time $u = t - r_{\text{obs}}^*$, in units of the orbital period of the center of the disk. Due to the finite location of the observer a vertical offset is present in the waveforms, induced by the matter sources in Eq. (2). This offset has been corrected for in the figure. The total mass accreted onto the black hole at the end of the simulations ($t = 100t_{\text{orb}}$) is $\sim 0.03M$ for model A and $\sim 2.20 \times 10^{-4}M$ for model B, which justifies the fixed spacetime approximation we use. The waveforms shown in the left panel of Fig. 1 indicate that the GW signals follow the torus oscillations. The decrease of the GW amplitude is determined by the amount of accreted mass. For model B the GW amplitude remains almost constant throughout the evolution, while for model A, where

more mass transfer is possible at the cusp, it decreases by $\sim 60\%$ after 100 orbital periods. As becomes evident on the right panel of the figure, which shows the corresponding energy spectra for both models, no black hole QNM is excited in the process. The spectra have been obtained after cutting out the first four periods of oscillation in order to avoid any contamination from the early time unphysical burst. At low frequencies (see the inset in the right panel of Fig. 1), distinctive peaks are visible, which correspond to the fluid p -modes of the disk, namely a fundamental mode f and a series of overtones [1, 15]. The fundamental $l = 2$ QNM of the black hole should lie at $2M\omega = 0.7473$ (indicated by a vertical dotted line in the plot), but the computed spectra show no hints of this mode. This is consistent with the results reported in [11] for the case of radial infall of quadrupolar shells, where it was shown that the fundamental QNM of the black hole is only significantly excited if the bulk of the maximum density of the (compact) shell reaches the peak of the Zerilli potential and if its typical linear dimensions are comparable with the width of the potential itself.

The absence of black hole QNM excitation in our simulations suggests that the gravitational waveforms should also be accurately computed by means of the Landau-Lifshitz quadrupole formula. We use our setup to assess the validity of the quadrupole formalism through a direct comparison with the gauge-invariant GWs extraction shown in Fig. 1. Since the quadrupole formula has been derived in a Newtonian framework, a number of approximations must be first considered in the transition to a general relativistic context. Let us consider a Minkowski background spacetime $\eta_{\hat{\mu}\hat{\nu}}$ ($\hat{\mu} = 0, 1, 2, 3$) and an axisymmetric GW source whose physical dimensions are much smaller than the reduced gravitational wave-

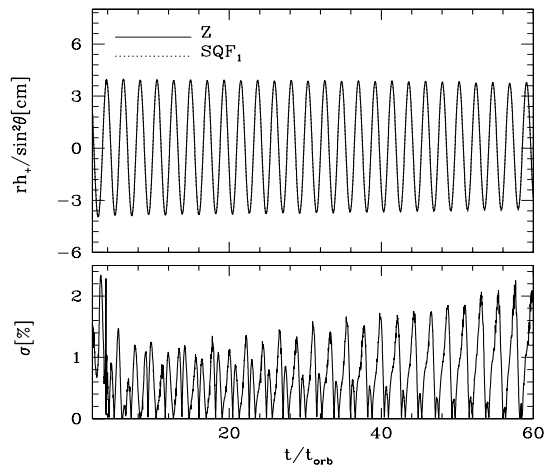


FIG. 2: Comparison between the $l = 2$ gravitational waveforms for model B extracted using the quadrupole formula SQF₁ (dotted line) and the gauge-invariant approach (solid line). The bottom panel shows the relative difference between the two normalized to the mean amplitude of the gauge-invariant method.

length (i.e. slow-motion approximation). In such case the only non-vanishing polarization amplitude of the wave is h_+ , which is given by [3, 6, 16]

$$h_+ = \frac{3 \sin^2 \theta}{2r} \frac{d^2 \mathcal{I}_{33}}{dt^2}, \quad (7)$$

where

$$\mathcal{I}_{\hat{i}\hat{j}} \equiv \int t^{\hat{0}\hat{0}} \left(x^{\hat{i}} x^{\hat{j}} - \frac{1}{3} \delta^{\hat{i}\hat{j}} r^2 \right) d^3x \quad (8)$$

becomes the reduced matter quadrupole moment tensor in the Newtonian limit $t^{\hat{0}\hat{0}} = \rho$ [16], ρ being the rest-mass density of the source. Eq. (7) is known as the Standard Quadrupole Formula (SQF) and can be used to extract GWs in a slow-motion nearly Newtonian regime. An extension of the simple Eqs. (7) and (8) to general relativity is problematic because the Einstein's equations are nonlinear in the background metric $g_{\mu\nu}$ [16]. However, since in the present physical context no black hole QNMs excitation is found, the nonlinear structure of the background metric, represented by the potential $V^{(e)}$, can be neglected in practice and the use of the quadrupole formula can be justified a posteriori. Following a pragmatic approach, a reasonable modification to account for general relativistic effects can be obtained by projecting t^{00} onto the local inertial frame of the tetrad associated with the stationary observers of the Schwarzschild space-time, so that $t^{\hat{0}\hat{0}} = \alpha^2 t^{00}$, where $t^{00} = \rho h u^0 u^0 + p g^{00}$ and $\alpha = \sqrt{-g_{00}}$ is the lapse. Here p is the pressure, $h = 1 + \varepsilon + p/\rho$ is the specific enthalpy, and ε is the specific internal energy of the fluid. Using spherical co-

ordinates we obtain

$$I = 2\pi \int_{-1}^1 dz \int_0^\infty (hDW - p) \left(\frac{3}{2} z^2 - \frac{1}{2} \right) r^4 dr, \quad (9)$$

where $I \equiv 3\mathcal{I}_{33}/2$, $z = \cos \theta$, $D = \rho W$ is the relativistic rest-mass density, and $W = \alpha u^0 = (1 - g_{ij}v^i v^j)^{-1/2}$ is the Lorentz factor. If we define $A_{20}^{E2} \equiv \sqrt{64\pi/15} d^2 I / dt^2$, the energy emitted in the quadrupole approximation is [5]

$$E = \frac{1}{32\pi^2} \int_0^\infty \omega^2 |\tilde{A}_{20}^{E2}(\omega, r)|^2 d\omega. \quad (10)$$

In the following we use SQF₁ to denote the standard quadrupole formula with the generalized quadrupole moment proposed above. Figure 2 displays the comparison, for model B, of the gravitational waveforms obtained with the Zerilli-Moncrief equation and with the SQF₁ definition for \mathcal{I}_{33} . The second time derivative has been computed directly from the numerical data using centered finite-differences. We note that for our particular physical setup and unlike the case of core collapse simulations [3, 5], the numerical noise associated with this procedure is negligible. Fig. 2 shows an excellent agreement between the two methods: the two lines perfectly overlap at early times and only small differences are reached after many orbital periods. Fig. 3 shows the corresponding comparison of the energy spectra for $t = 100t_{\text{orb}}$ and (in the inset) a close up of the waveforms for different alternative definitions of $t^{\hat{0}\hat{0}}$. The Newtonian SQF ($t^{\hat{0}\hat{0}} = \rho$) slightly underestimates the wave amplitude while SQF₂ ($t^{\hat{0}\hat{0}} = \rho W$) is closer to the gauge-invariant signal; SQF₃, corresponding to $t^{\hat{0}\hat{0}} = \rho u^0$ and used in Refs. [2, 6, 17], gives the worst relative agreement in the present physical context (dash-dotted line in the inset of Fig. 3).

To quantify the differences among the various alternative expressions we use for the quadrupole moment we report in Table II the relative errors ΔE^{20} found in the total energy emitted after the frequency integration of the power spectra for all four models of our sample. We recall that from model A to D the radial location of the center of the disk increases gradually. It is found that the SQF₁ (fourth column in Table II) gives the best agreement with the gauge-invariant GW extraction, with an error that is always less than 2%. On the other hand, the SQF₃ yields the worst result for either model, systematically overestimating the amplitude of the waveforms, the reason being that, when compared to the other expressions, the functional form of SQF₃ contains a division by an extra lapse function ($\alpha < 1$).

It needs to be mentioned, however, that the decrease in ΔE^{20} with increasing r_{center} , observed in SQF and SQF₃ in Table II, seems accidental. This has been checked by analyzing additional models with the same linear dimension but with the center located at $r_{\text{center}} = 10.17$ and $r_{\text{center}} = 10.47$. The latter is the maximum allowed value for a closed disk with $l = 4$ [14]. No clear continuation in the trend in ΔE^{20} reported in Table II

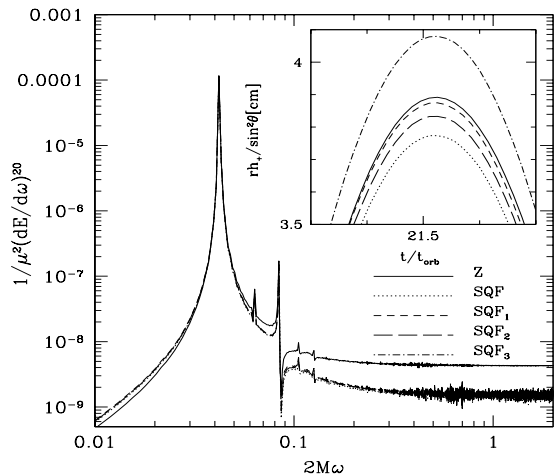


FIG. 3: Comparison of the energy spectra for model B and a portion of the waveform when different definitions of the generalized quadrupole moment of the torus are used.

TABLE II: Relative differences $\Delta E^{20} = |E^{20} - E|/E^{20}$ among the emitted energies computed using different versions of the quadrupole formula (E) and the gauge-invariant approach (E^{20}) for disk models with different position of the center.

Model	r_{center}	$\Delta E_{\text{SQF}}^{20}$	$\Delta E_{\text{SQF}_1}^{20}$	$\Delta E_{\text{SQF}_2}^{20}$	$\Delta E_{\text{SQF}_3}^{20}$
A	7.720	2.9%	0.7%	0.8%	11.0%
B	7.720	5.9%	0.3%	2.6%	10.6%
C	8.352	4.9%	1.8%	3.2%	6.7%
D	9.971	2.7%	1.7%	2.2%	3.8%

has been found for these additional models. The largest errors computed appear in SQF₃ for the model with $r_{\text{center}} = 10.17$ ($\Delta E^{20} \sim 5.4\%$) and in SQF for the model with $r_{\text{center}} = 10.47$ ($\Delta E^{20} \sim 5\%$).

Further evidence on the sensitivity of these results on the model properties is gained by reducing the potential gap in model D to $\Delta W = -0.008$, keeping the center at the same location. As a result the disk becomes much larger, extending from $r_{\text{in}} = 4.93$ to $r_{\text{out}} = 42.5$. In this case, the relative difference in the emitted energy between the gauge-invariant waveform and the quadrupole formula can be as large as $\sim 25\%$ for SQF, SQF₁ and SQF₂, while $\Delta E^{20} \sim 21\%$ for SQF₃. Following Tanaka *et al.* [10], who computed GWs from particles orbiting around a Schwarzschild black hole using linear perturbation theory, we interpret this disagreement for enlarged tori as the result of GWs back-scattering with the tail of the background potential.

As mentioned above, in simulations of core collapse [3, 5], the accurate numerical computation of the time derivatives appearing in the SQF is prone to introduce high-frequency numerical noise. The common procedure to circumvent this is to rewrite Eq. (7) making use of

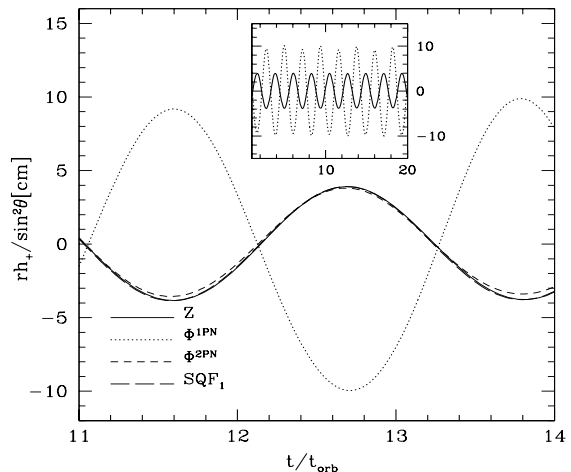


FIG. 4: Model B: comparison between the Zerilli-Moncrief function, the SQF₁ and the SF for different choices of the potential Φ . The inset shows more periods of oscillations.

the Newtonian limit of the general relativistic hydrodynamics equations (i.e. the Euler and continuity equations) [2, 18] to eliminate the time derivatives. In axisymmetry the resulting expression reads

$$\begin{aligned}
 A_{20}^{E2} = & k \int_{-1}^1 dz \int_0^\infty \rho \left[v_r v^r (3z^2 - 1) \right. \\
 & + v_\theta v^\theta (2 - 3z^2) - v_\varphi v^\varphi - 6z \sqrt{(v_r v_r)(v_\theta v_\theta)(1 - z^2)} \\
 & \left. - r \partial_r \Phi (3z^2 - 1) + 3z \partial_\theta \Phi \sqrt{1 - z^2} \right] r^2 dr, \quad (11)
 \end{aligned}$$

where $k = 16\pi^{3/2}/\sqrt{15}$ and Φ is the Newtonian gravitational potential generated by the central source M . This equation is known as the *stress formula* (SF), and it has been applied in diverse astrophysical scenarios [1, 5, 18]. Since Eq. (11) is obtained from the Newtonian fluid equations, its application in a general relativistic code poses some ambiguities. However, it is possible to introduce suitable forms for Φ in Eq. (11) to obtain results which are consistent with those derived in the perturbative framework. An elementary possibility is to use a first post-Newtonian (1PN) expression for Φ , as it was done in [1]. In practice Φ can be obtained from $g_{rr} = 1 - 2\Phi$ which is correct at 1PN [19]; i.e. $\Phi \equiv \Phi^{1\text{PN}} = -M/(r - 2M)$. Moreover, one can also introduce the first terms of the 2PN expansion of g_{rr} [19], solving the quadratic equation $g_{rr} = 1 - 2\Phi + 2\Phi^2$ and choosing the solution which recovers the Newtonian potential $\Phi^{\text{N}} = -M/r$ for large r ; i.e. $\Phi \equiv \Phi^{2\text{PN}} = 1/2 \left[1 - \sqrt{(r + 2M)/(r - 2M)} \right]$. Figure 4 shows the GW signals for model B computed using the SQF₁ (long-dashed line), the Zerilli-Moncrief function Z (solid line), and the SF with $\Phi^{1\text{PN}}$ (dotted line) or $\Phi^{2\text{PN}}$ (short-dashed line). The waveforms obtained from the SF present a systematic global vertical offset [1]

which was corrected in the figure. Figure 4 shows that a good agreement is found among all waveforms except for those computed using $\Phi^{1\text{PN}}$. In this case, the signal is out of phase by half a period, due to the $\partial_r\Phi$ term being dominant in Eq. (11) and thus responsible for a change of sign, while the amplitude is about a factor of two larger than that of the other waveforms. On the other hand, it is remarkable the good agreement in amplitude found among the SF waveform using $\Phi^{2\text{PN}}$ with both the Zerilli-Moncrief equation and the SQF₁. We finally note that the use of a potential consistent with the Schwarzschild metric, obtained from $g_{00} = \exp(-2\Phi)$, results in a signal whose amplitude is $\sim 30\%$ larger than the one obtained with SQF₁. This stresses the intrinsic ambiguity which relies in the use of a modified Newtonian formula in a general relativistic context. Work is in progress to derive a modified stress formula which holds in this regime.

In this paper we have studied the GW signals driven by oscillations of thick accretion disks around a Schwarzschild black hole by means of gauge-invariant metric perturbation theory and modifications of the SQF. The comparison between the two approaches used has been discussed in detail. For the models considered, the GW signal has been found to be mainly determined by the matter flows and no evidence of black hole QNM excitation has been observed.

We thank P. Cerdá-Durán, V. Ferrari, L. Gualtieri, J.A. Pons, M. Portilla, and L. Rezzolla for useful discussions. This work has been supported by the Angelo Della Riccia Foundation, the Spanish MEC (SB2002-0128), and the Spanish MCyT (grant AYA 2001-3490-C02-01). The computations were performed on the Beowulf Cluster for Numerical Relativity *Albert100*, at the University of Parma.

-
- [1] O. Zanotti, L. Rezzolla, and J.A. Font, *Mon. Not. R. Astron. Soc.* **341**, 832 (2003); O. Zanotti, J.A. Font, L. Rezzolla, and P.J. Montero, *ibid.* **356**, 1371 (2005).
 - [2] L. Blanchet, T. Damour and G. Schäfer, *Mon. Not. R. Astron. Soc.* **242**, 289 (1990).
 - [3] S.L. Finn and C.R. Evans, *Astrophys. J.* **351**, 588 (1990).
 - [4] T. Zwerger and E. Müller, *Astron. Astrophys.* **320**, 209 (1997).
 - [5] H. Dimmelmeier, J.A. Font, and E. Müller, *Astron. Astrophys.* **393**, 523 (2002).
 - [6] M. Shibata and Y.I. Sekiguchi, *Phys. Rev. D* **68**, 104020 (2003).
 - [7] T. Regge and J.A. Wheeler, *Phys. Rev.* **108**, 1063 (1957).
 - [8] F.J. Zerilli, *Phys. Rev. D* **2**, 2141 (1970).
 - [9] V. Moncrief, *Ann. Phys. (N.Y.)* **88**, 323 (1974).
 - [10] T. Tanaka, M. Shibata, M. Sasaki, H. Tagoshi, and T. Nakamura, *Prog. Theor. Phys.* **90**, 65 (1993).
 - [11] A. Nagar, G. Diaz, J.A. Pons, and J.A. Font, *Phys. Rev. D* **69**, 124028 (2004).
 - [12] A. Nagar and L. Rezzolla, arXiv:gr-qc/0502064 (2005).
 - [13] U.H. Gerlach and U.K. Sengupta, *Phys. Rev. D* **19**, 2268 (1979); C. Gundlach and J.M. Martín-García, *ibid.* **61**, 084024 (2000).
 - [14] J.A. Font and F. Daigne, *Mon. Not. R. Astron. Soc.* **334**, 383 (2002); F. Daigne and J.A. Font, *ibid.* **349**, 841 (2004).
 - [15] L. Rezzolla, S. Yoshida, and O. Zanotti, *Mon. Not. R. Astron. Soc.* **344**, 978 (2003).
 - [16] C.W. Misner, K.S. Thorne, and J.A. Wheeler, *Gravitation*, Freeman (1973).
 - [17] H. Dimmelmeier, J. Novak, J.A. Font, J.M. Ibañez, and E. Müller, *Phys. Rev. D* **71**, 064023 (2005).
 - [18] L.S. Finn, in *Frontiers in Numerical Relativity*, ed. C.R. Evans, L.S. Finn, and D.W. Hobill, Cambridge University Press, Cambridge, England 1989.
 - [19] L. Blanchet, *Living Rev. Relativ.* **3**, (2002).